JOURNAL OF VIROLOGY, Nov. 2000, p. 10801–10806 Vol. 74, No. 22
0022-538X/00/$04.00+0

Rotavirus Infection Induces Cytoskeleton Disorganization in Human Intestinal Epithelial Cells: Implication of an Increase in Intracellular Calcium Concentration

JEAN-PHILIPPE BRUNET,* NATHALIE JOURDAN, JACQUELINE COTTE-LAFFITTE, CATHERINE LINXE, MONIQUE GÉNITEAU-LEGENDRE, ALAIN SERVIN, AND ANNE-MARIE QUÉRO

Institut National de la Santé et de la Recherche Médicale, Unité 510, Pathogènes et Fonctions des Cellules Épithéliales Polarisées, Faculté de Pharmacie, Université Paris XI, 92296 Châtenay-Malabry cedex, France

Received 25 May 2000/Accepted 23 August 2000

Rotavirus infection is the most common cause of severe infantile gastroenteritis worldwide. In vivo, rotavirus exhibits a marked tropism for the differentiated enterocytes of the intestinal epithelium. In vitro, differentiated and undifferentiated intestinal cells can be infected. We observed that rotavirus infection of the human intestinal epithelial Caco-2 cells induces cytoskeleton alterations as a function of cell differentiation. The vimentin network disorganization detected in undifferentiated Caco-2 cells was not found in fully differentiated cells. In contrast, differentiated Caco-2 cells presented Ca^{2+}-dependent microtubule disassembly and Ca^{2+}-independent cytokeratin 18 rearrangement, which both require viral replication. We propose that these structural alterations could represent the first manifestations of rotavirus-infected enterocyte injury leading to functional perturbations and then to diarrhea.

Rotaviruses, members of the *Reoviridae* family, are recognized as the most important cause of viral gastroenteritis in young children. Although much is known about their replication and maturation processes, the pathophysiologic mechanisms by which rotavirus infection induces diarrhea remain unclear. Cytoskeleton alterations could be an important stage in rotavirus-induced intestinal epithelial cell injury. Several studies have described the interactions of rotavirus with the cytoskeleton in MA104 (13, 24), CV-1 (40), or BHK21 (27) unpolarized cell lines. Cytoskeleton alteration was also observed in a rotavirus-infected neuronal cell line (41). Whereas the cells on the sides of microvilli, which do not totally display the morphologic and functional characteristics of mature enterocytes, can be infected by rotavirus, mature enterocytes on tips of the villi constitute the human rotavirus main target cells (8, 9). In order to approach the in vivo situation and to gain further insights into the pathophysiologic mechanisms of rotavirus infection, we and others have used the human intestinal epithelial cell lines Caco-2 (5, 15, 17, 35) and HT-29 (6, 21, 30, 33, 34). Since rotavirus can infect both undifferentiated and differentiated Caco-2 cells (16, 18, 35), this cell line, which spontaneously differentiates in culture, represents, like HT-29 cells, an attractive model to study the mechanisms of pathogenicity of rotavirus as a function of cell differentiation. It was reported by Michelangeli et al. (25) that the OSU strain of porcine rotavirus leads to an elevation in intracellular calcium concentration ($[Ca^{2+}]_i$) in MA104 cells. Using differentiated Caco-2 cells, which display many of the morphological and functional properties of mature enterocytes (22, 31), we recently reported that the simian rhesus rotavirus strain RRV induces an increase in $[Ca^{2+}]_i$ which is responsible for microvillar F-actin disassembly (5). This alteration is concomitant with a decrease in the activity and apical expression of the brush border-associated hydrolase sucrase-isomaltase (SI), which results from a profound perturbation in the intracellular traffic of the enzyme (15). The Caco-2 cell cytoskeleton plays a central role in the intracellular traffic of functional molecules and in the development and maintenance of intestinal functions (7, 10, 23, 32, 43). Therefore, we hypothesize that cytoskeleton alterations could be implicated in functional perturbations of enterocytes, leading to impaired nutrient digestion and thereby indirectly participating in the triggering of diarrhea. In previous works, we and colleagues studied the impact of RRV infection on actin microfilament organization (5, 15). In the present work, using confocal laser scanning microscopy, we studied in undifferentiated and differentiated Caco-2 cells the impact of RRV infection on the distribution of the two other types of protein filaments that form the cytoskeleton: (i) microtubules, which are implicated in vesicle and organelle transport and in cell polarization, and (ii) intermediate filaments, which give cells mechanical strength by spanning the cytoplasm from one cell-to-cell junction to another (19). We studied the impact of RRV infection on cytokeratin 18 (CK18) and vimentin, which are members of the two classes of cytoplasmic intermediate filaments present in Caco-2 cells (3). We next investigated if the increase in $[Ca^{2+}]_i$ is responsible for the cytoskeleton alterations observed in RRV-infected differentiated Caco-2 cells.

RRV rotavirus, obtained from J. Cohen (INRA, Jouy-en-Josas, France), was propagated and its titers were determined in MA104 cells (from J. Cohen) as previously described (15). Viral titers were expressed as log PFU/ml. Caco-2 cells (passages 60 to 90) were grown as previously described (15). Caco-2 cells (from A. Zweibaum, INSERM, Paris, France) were seeded (10^4/cm^2) on tissue culture-treated polycarbonate Transwell filters (Costar) containing pores of 0.4-μm diameter or in 24-well plates (TPP; PolyLabo, Strasbourg, France) containing coverslips. Transepithelial electrical resistance (TER) of the Caco-2 cell monolayer was measured with a Millicell-ERS apparatus (Millipore S.A., Saint Quentin en Yvelines, France). Undifferentiated (5 days after seeding) or fully differ-

* Corresponding author. Mailing address: INSERM U-510, Faculté de Pharmacie, 5 rue J. B. Clément, 92296 Châtenay-Malabry cedex, France. Phone: 33-1 46 83 55 24. Fax: 33-1 46 83 58 83. E-mail: jean-philippe.brunet@cep.u-psud.fr.

entiated (14 days after seeding) Caco-2 cells were infected with trypsin-activated RRV at a multiplicity of infection of 10, as previously described (5). Caco-2 cells were fixed with 2% paraformaldehyde at the indicated time postinfection (p.i.). After washing in phosphate-buffered saline containing 0.2% Tween 20, the cells were permeabilized using Triton X-100 and incubated with anti-β-tubulin monoclonal antibody (MAb) TUB 2.1 (immunoglobulin G1 [IgG1] from Sigma; working dilution, 1:200), anti-CK18 MAb CY-90 (purified IgG1 from Sigma; working dilution, 1:100), anti-vimentin MAb VIM-13.2 (IgM from Sigma; working dilution, 1:200), or rat anti-human SI MAb 8A9 (from S. Maroux, INSERM, Marseille, France; working dilution, 1:200). Caco-2 cells were then washed and incubated with fluorescein isothiocyanate-conjugated anti-mouse or anti-rat IgG (Jackson ImmunoResearch via Interchim, Montluçon, France). Double immunofluorescence was performed with rabbit anti-rotavirus polyclonal antibody prepared with RF bovine rotavirus strain (from J. Cohen; working dilution, 1:1,000), which recognizes only structural proteins of rotavirus group A, followed by incubation with tetramethyl rhodamine isothiocyanate-conjugated anti-rabbit IgG (Jackson ImmunoResearch). Specificity of labeling and absence of signal crossover were established by examination of single-labeled control samples. Fluorescence was examined by confocal laser scanning microscopy using a krypton-argon laser on a LEICA TCS equipped with a DMR inverted microscope and a 63/1.4 objective (×63 magnification with a 1.4 numerical aperture). Genetic inactivation of RRV was accomplished using psoralen and long-wave UV light that irreversibly cross-links viral RNA (12). The effectiveness of psoralen-UV inactivation and the preservation of viral structure and viral masses after the inactivation were investigated as previously described (5) (data not shown). $[Ca^{2+}]_i$ was measured as previously described (5), using the fluorescent indicator quin2-AM. Fluorescence was measured in a Perkin-Elmer LS-50 spectrofluorimeter with the excitation and emission wavelengths being recorded at 339 and 492 nm, respectively, in a thermostatically controlled quartz cuvette (37°C) equipped with a magnetic microstirrer. $[Ca^{2+}]_i$ was evaluated by the method of Tsien et al. (39) as previously described (5). Autofluorescence was constant throughout each measurement and did not affect $[Ca^{2+}]_i$ calculation. Caco-2 cell membrane integrity was investigated by measuring the lactate dehydrogenase (LDH) activity in the culture medium with an Enzyline LDH kit (Biomerieux, Craponne, France), according to the manufacturer's instructions. As previously reported (5, 15), the cell integrity was not modified in any of the experiments conducted until 24 h p.i. (data not shown). Values are given as means ± standard deviations, and statistical differences were determined by Student's *t* test.

The state of differentiation of Caco-2 cells was examined by immunofluorescence evaluation of the brush border expression of SI and by evaluating polarization through measurement of TER (11). Five days after seeding, only weak staining was observed at the apical domain of Caco-2 cells (Fig. 1a), indicating an undifferentiated pattern. Fourteen days after seeding, intensive SI expression characteristic of a fully differentiated pattern was observed (Fig. 1b). TER was 135 $\Omega \cdot cm^2$ for undifferentiated Caco-2 cells. It reached 800 $\Omega \cdot cm^2$ at day 14, confirming the polarization of the whole monolayer, and did not significantly vary after this time.

The microtubular organization was first studied (Fig. 1c to j). Fig. 1e, h, and j show viral antigen staining in the same cells as in Fig. 1d, g, and i. In undifferentiated Caco-2 cells (Fig. 1c to e), the microtubules were seen surrounding the nucleus of control cells (Fig. 1c) and along the cell extensions. No change was seen in RRV-infected cells until 24 h p.i. (Fig. 1d). In differentiated Caco-2 cells (Fig. 1f to j), no change in microtubule organization was seen in RRV-infected cells until 18 h p.i. In contrast, at 18 h p.i. and beyond this time, only weak staining of β-tubulin could be observed in the place of the lateral network (Fig. 1g), as compared with the control cells (Fig. 1f), indicating a dramatic disassembly of the microtubule network. It is now well documented that $[Ca^{2+}]_i$ elevation leads to microtubule destabilization by inhibiting the assembly and by inducing the disassembly of these filaments (4, 28, 29, 38, 42). We have previously shown that RRV infection of Caco-2 cells induces a progressive increase in $[Ca^{2+}]_i$ from 7 h p.i., with maximal values reached at 18 h p.i. (5). We confirmed that the average $[Ca^{2+}]_i$ was 446 ± 16 nM ($n = 6$) in infected cells 18 h p.i. versus 140 ± 5 nM ($n = 6$) in uninfected cells (significantly different; $P < 0.01$) (Table 1). To determine the involvement of a $[Ca^{2+}]_i$ rise in microtubule disassembly, we examined the effects of extra- and intracellular Ca^{2+} depletion on β-tubulin alteration in RRV-infected Caco-2 cells. At 14 h p.i., culture medium was removed and infected cells were incubated for 4 h in fresh medium without Ca^{2+} containing 25 μM 1,2-bis(2-aminophenoxy)ethan-*N*,*N*,*N*′,*N*′-tetraacetic acid acetoxymethyl ester (BAPTA-AM; Sigma) to chelate intracellular Ca^{2+}. Ca^{2+} depletion reduced to the last 4 h of infection was chosen because of the absence of effect on virus replication (7.26 ± 0.35 in treated cells versus 7.48 ± 0.61 in untreated cells; not significantly different [$P > 0.01$]; $n = 3$). This treatment totally abolished the RRV-induced $[Ca^{2+}]_i$ rise observed at 18 h p.i. (126 ± 9 nM; not significantly different from control cells [$P > 0.01$]; $n = 3$) (Table 1) and RRV-induced microtubule disassembly (Fig. 1i). In infected, mock-treated cells, the change of medium containing Ca^{2+} at 14 h p.i. did not affect $[Ca^{2+}]_i$ increase or microtubule disassembly (data not shown) and was used as a control. These results suggest that rotavirus-induced increase in $[Ca^{2+}]_i$ is necessary for β-tubulin disorganization.

The organization of intermediate filaments was studied by immunofluorescence labeling of CK18 (Fig. 2a to h) and vimentin (Fig. 2i to n). Fig. 2c, f, h, k, and n show viral antigen staining in the same cells as in Fig. 2b, e, g, j, and m. In undifferentiated cells (Fig. 2a to c), CK18 appeared as a dense network of thin filaments surrounding the nucleus and extended out into the cytoplasm in control (Fig. 2a) as well as in RRV-infected cells (Fig. 2b). In differentiated cells (Fig. 2d to h), CK18 staining appeared in control cells (Fig. 2d) as pericellular structures all around the basolateral membrane corresponding to the tonofilaments. In differentiated RRV-infected cells, no change was observed until 18 h p.i. In contrast, at 18 h p.i. and beyond this time, the CK18 was detected in cytoplasmic vesicular structures mainly located near the basolateral membrane (Fig. 2e). As elevated Ca^{2+} concentrations have been shown to potentialize intermediate filament proteolysis (20) and phosphorylation (14, 44), we examined the impact of Ca^{2+} depletion on rotavirus-induced CK18 alteration. Treatment of infected cells from 14 to 18 h p.i. with medium without Ca^{2+} containing BAPTA-AM did not prevent formation of vesicular structures (Fig. 2g), indicating that rotavirus-induced CK18 alteration is Ca^{2+} independent. In undifferentiated Caco-2 cells (Fig. 2i to k), vimentin showed distribution throughout the cytoplasm of control cells (Fig. 2i) in the form of a close system of filaments surrounding the nucleus. In infected cells at 18 h p.i. and beyond, the irregular pattern of vimentin distribution appeared: a condensation of vimentin staining in vesicular structures associated with the emergence of several zones without staining throughout the cytoplasm could be observed (Fig. 2j). In contrast, in differentiated cells (Fig. 2l to n), no

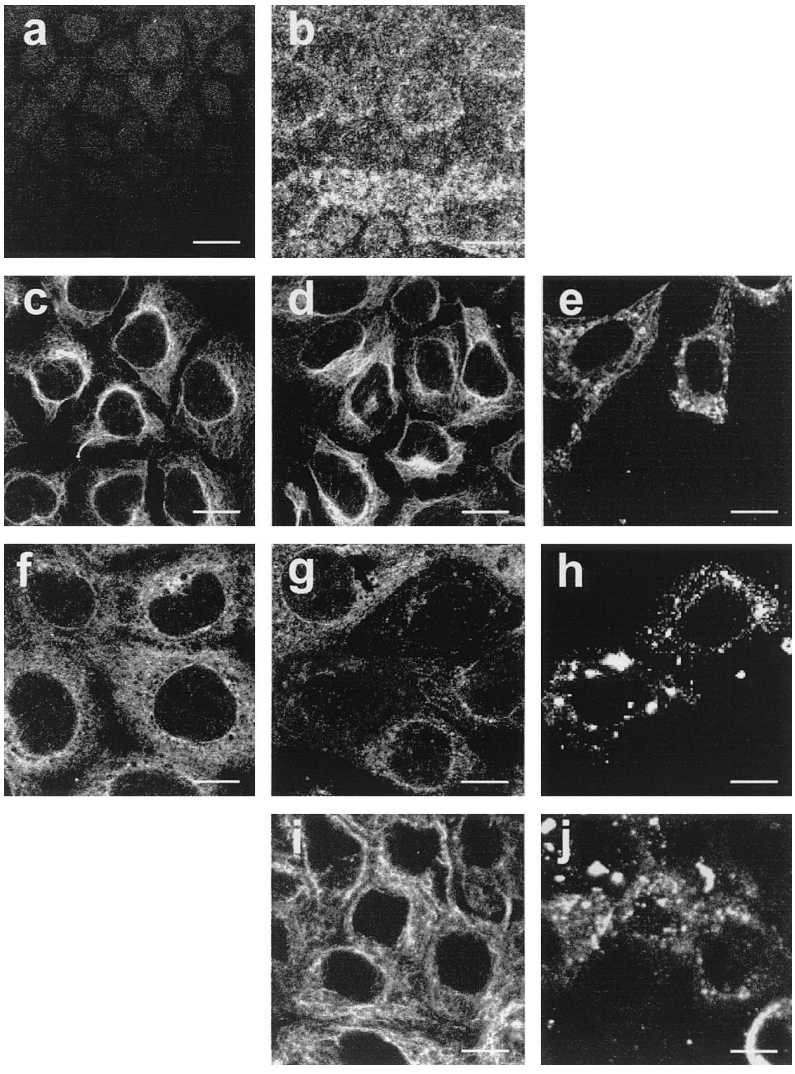

FIG. 1. SI expression at the apex of undifferentiated (a) and differentiated (b) Caco-2 cells. Horizontal sections were generated by confocal laser scanning microscopy along an axis perpendicular to the monolayer. Microtubule organization as revealed by anti-β-tubulin antibody in Caco-2 cells is shown. (c, d, f, g) Identical pattern of microtubule network in control (c) and RRV-infected (d) undifferentiated cells at 24 h p.i.; tubulin staining in control differentiated Caco-2 cells (f); lateral microtubule disassembly in RRV-infected Caco-2 cells at 18 h p.i. (g). Incubation of RRV-infected cells from 14 to 18 h p.i. in culture medium without Ca^{2+} containing 25 μM BAPTA-AM totally protects Caco-2 cells from microtubule alteration (i). Panels e, h, and j show viral antigen staining in the same cells as presented in panels d, g, and i. Bars, 10 μM.

change was found in RRV-infected cells until 24 h p.i. (Fig. 2m), as compared with the control cells (Fig. 2l).

The addition of nonreplicating viral particles to Caco-2 cells did not induce any perturbation in β-tubulin, CK18, or vimentin distribution, even after 24 h of contact (data not shown), indicating that viral protein synthesis is necessary to induce cytoskeleton alteration in fully differentiated, as in undifferentiated, Caco-2 cells.

We have demonstrated here that rotavirus replication induces cytoskeleton alterations of Caco-2 cells as a function of cell differentiation. As we previously described for microvillar F-actin disassembly (5), our results show that rotavirus-induced $[Ca^{2+}]_i$ increase is responsible for microtubule alteration in differentiated Caco-2 cells, indicating that perturbation in Ca^{2+} homeostasis is largely implicated in rotavirus-induced enterocyte injury. These results could help to explain the RRV-induced apical alteration in SI distribution, which was described previously (15). It is well established that in Caco-2 cells, microtubule disruption induces delays in the appearance of apical membrane glycoproteins such as SI and leads to a partial missorting to the basolateral surface (1, 10). Consequently, the Ca^{2+}-dependent disassembly of the microtubule network we observed upon RRV infection could play a role in the impair-

TABLE 1. Intracellular calcium concentration in Caco-2 cells

Treatment	Intracellular calcium concn (nM)[a]	No. of expts
Control cells	140 ± 5	6
RRV-infected cells at 18 h p.i.	446 ± 16[b]	6
RRV-infected cells incubated in medium without Ca^{2+} containing 25 μM BAPTA-AM from 14 to 18 h p.i.	126 ± 9[c]	3

[a] Values are means ± standard deviations.
[b] Significantly different ($P < 0.01$). Statistical differences between control and RRV-infected cells were determined by Student's *t* test.
[c] Not significantly different ($P > 0.01$).

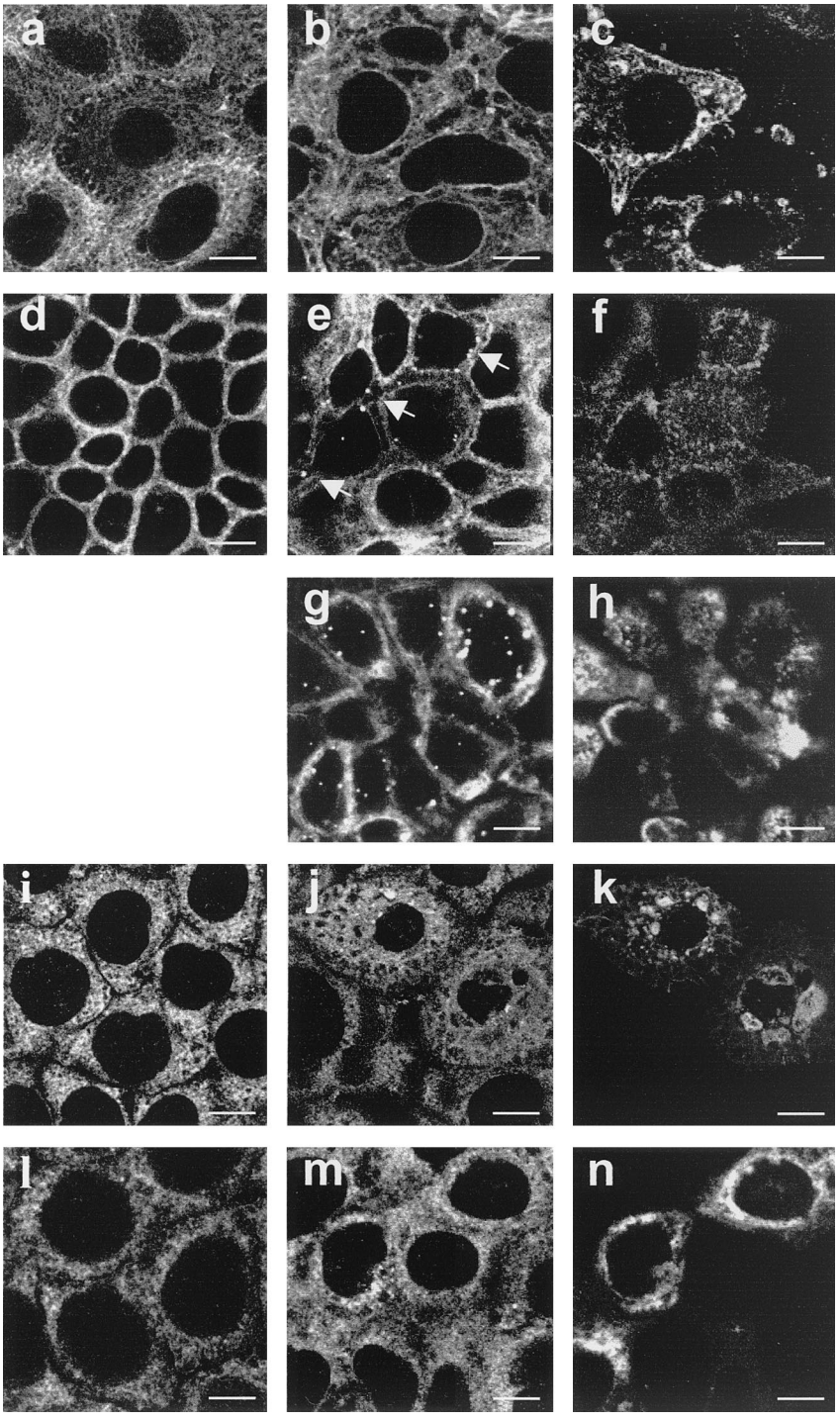

FIG. 2. Organization of intermediate filaments in Caco-2 cells. (a, b, d, and e) CK18 staining of control (a) and RRV-infected (b) undifferentiated cells at 24 h p.i.; peripheral staining corresponding to the tonofilaments in uninfected differentiated cells (d); presence of vesicular structures in RRV-infected differentiated cells at 18 h p.i. (e, arrows). Incubation of RRV-infected cells from 14 to 18 h p.i. in culture medium without Ca^{2+} containing 25 μM BAPTA-AM did not protect Caco-2 cells from CK18 alteration (g). (i, j, l, m) Vimentin staining of control (i) and altered network in RRV-infected (j) undifferentiated cells at 18 h p.i.; control (l) and RRV-infected (m) differentiated cells at 24 h p.i. Panels c, f, h, k, and n show viral antigen staining in the same cells as presented in panels b, e, g, j, and m. Bars, 10 μM.

ment of SI delivery to the apical domain. It was reported that the rotavirus nonstructural protein NSP4 induces $[Ca^{2+}]_i$ increase when expressed in or added to Sf9 cells (36, 37) and induces diarrhea when administered to young mice, probably through Ca^{2+}-dependent chloride secretion (2, 26). Our results indicate that $[Ca^{2+}]_i$ increase could also participate in triggering and/or amplifying diarrhea through the induction of cytoskeleton disassembly, which may induce perturbations of the expression of intestinal hydrolases leading to impairment of nutrient digestion.

We showed that RRV infection promotes vesicular distribution of CK18 in differentiated Caco-2 cells. A similar pattern,

associated with hyperphosphorylation, has been observed for cytokeratin 19 after the treatment of Caco-2 cells with the adenyl cyclase agonist forskolin (3). CK18 hyperphosphorylation has also been shown after heat stress or rotavirus infection of the human epithelial colon cell line HT29 (21). Thus, our results suggest an increase in CK18 phosphorylation upon rotavirus infection of Caco-2 cells. Since it has been shown that downregulation of cytokeratin 19 in Caco-2 cells leads to the disorganization of the apical actin and tubulin networks and also perturbs the apical targeting of SI (32), the alteration in CK18 distribution we observed upon RRV infection could also participate in the apical cytoskeleton network disassembly, thereby explaining the block in apical SI delivery.

In undifferentiated Caco-2 cells, we showed that RRV induces only vimentin alteration, as in RRV-infected unpolarized CV-1 cells (40). These results suggest that the infection of undifferentiated cells could also participate in rotavirus pathogenesis through structural perturbations.

In conclusion, since the RRV-induced structural alterations occur in the absence of cell destruction, we propose that they could represent the first manifestations of rotavirus-infected enterocyte injury leading to functional perturbations and then to diarrhea.

This work was supported by a French Ministry of Research grant from the Réseau de Recherche sur les Gastro-entérites à Rotavirus: Epidémiologie, Structure et Interaction avec l'hôte.

We thank J. Cohen (INRA, Jouy-en-Josas) for kindly providing antirotavirus serum and the RRV strain. Confocal experiments were performed with the kind cooperation of P. Fontanges and the Institut Fédératif de Recherche 65 INSERM.

REFERENCES

1. **Achler, C., D. Filmer, C. Merte, and D. Drenckhahn.** 1989. Role of microtubules in polarized delivery of apical membrane proteins to the brush border of the intestinal epithelium. J. Cell Biol. **109:**179–189.
2. **Ball, J. M., P. Tian, C. Q.-Y. Zeng, A. P. Morris, and M. K. Estes.** 1996. Age-dependent diarrhea induced by a rotaviral nonstructural glycoprotein. Science **272:**101–104.
3. **Baricault, L., B. D. Néchaud, C. Sapin, P. Codogno, P. Denoulet, and G. Trugnan.** 1994. The network organization and the phosphorylation of cytokeratins are concomitantly modified by forskolin in the enterocyte-like differentiated Caco-2 cell line. J. Cell Sci. **107:**2909–2918.
4. **Berkowitz, S. A., and J. Wolff.** 1981. Intrinsic calcium sensitivity of tubulin polymerization. The contributions of temperature, tubulin concentration, and associated proteins. J. Biol. Chem. **256:**11216–11223.
5. **Brunet, J. P., J. Cotte-Laffitte, C. Linxe, A. M. Quero, M. Geniteau-Legendre, and A. Servin.** 2000. Rotavirus infection induces an increase in intracellular calcium concentration in human intestinal epithelial cells: role in microvillar actin alteration. J. Virol. **74:**2323–2332.
6. **Casola, A., M. K. Estes, S. E. Crawford, P. L. Ogra, P. B. Ernst, R. P. Garofalo, and S. E. Crowe.** 1998. Rotavirus infection of cultured intestinal epithelial cells induces secretion of CXC and CC chemokines. Gastroenterology **114:**947–955.
7. **Costa de Beauregard, M.-A., E. Pringault, S. Robine, and D. Louvard.** 1995. Suppression of villin expression by antisense RNA impairs brush border assembly in polarized epithelial intestinal cells. EMBO J. **14:**409–421.
8. **Davidson, G. P., I. Goller, R. F. Bishop, R. R. W. Townley, I. H. Holmes, and B. J. Ruck.** 1975. Immunofluorescence in duodenal mucosa of children with acute enteritis due to a new virus. J. Clin. Pathol. **28:**263–266.
9. **Flewett, T. H., and G. N. Woode.** 1978. The rotaviruses. Arch. Virol. **57:**1–23.
10. **Gilbert, T., A. LeBivic, A. Quaroni, and E. Rodriguez-Boulan.** 1991. Microtubular organization and its involvement in the biogenetic pathways of plasma membrane proteins in Caco-2 intestinal epithelial cells. J. Cell Biol. **113:**275–288.
11. **Grasset, E., M. Pinto, E. Dussaulx, A. Zweibaum, and J. F. Desjeux.** 1984. Epithelial properties of human colonic carcinoma cell line Caco-2: electrical parameters. Am. J. Physiol. **247:**C260–C267.
12. **Groene, W. S., and R. D. Shaw.** 1992. Psoralen preparation of antigenically intact noninfectious rotavirus particles. J. Virol. Methods **38:**93–102.
13. **Hua, J., and J. Patton.** 1994. The carboxyl-half of the rotavirus nonstructural protein NS53 (NSP1) is not required for virus replication. Virology **198:**567–576.
14. **Inagaki, N., H. Goto, M. Ogawara, Y. Nishi, S. Ando, and M. Inagaki.** 1997. Spatial patterns of Ca^{2+} signals define intracellular distribution of a signaling by Ca^{2+}/calmodulin-dependent protein kinase II. J. Biol. Chem. **272:**25195–25199.
15. **Jourdan, N., J.-P. Brunet, C. Sapin, A. Blais, J. Cotte-Laffitte, F. Forestier, A.-M. Quero, G. Trugnan, and A. Servin.** 1998. Rotavirus infection reduces sucrase-isomaltase expression in human intestinal epithelial cells by perturbing protein targeting and organization of microvillar cytoskeleton. J. Virol. **72:**7228–7236.
16. **Jourdan, N., J. Cotte-Laffitte, F. Forestier, A. L. Servin, and A. M. Quero.** 1995. Infection of cultured human intestinal cells by monkey RRV and human Wa rotavirus as a function of intestinal epithelial cell differentiation. Res. Virol. **146:**325–331.
17. **Jourdan, N., M. Maurice, D. Delautier, A. M. Quero, A. L. Servin, and G. Trugnan.** 1997. Rotavirus is released from the apical surface of cultured human intestinal cells through nonconventional vesicular transport that bypasses the Golgi apparatus. J. Virol. **71:**8268–8278.
18. **Kitamoto, N., R. F. Ramig, D. O. Matson, and M. K. Estes.** 1991. Comparative growth of different rotavirus strains in differentiated cells (MA104, HepG2, and Caco-2). Virology **184:**729–737.
19. **Ku, N. O., X. Zhou, D. M. Toivola, and M. B. Omary.** 1999. The cytoskeleton of digestive epithelia in health and disease. Am. J. Physiol. **277:**G1108–G1137.
20. **Lazarides, E.** 1982. Intermediate filaments: a chemically heterogeneous, developmentally regulated class of proteins. Annu. Rev. Biochem. **51:**219–250.
21. **Liao, J., L. A. Lowthert, and M. Bishr Omary.** 1995. Heat stress or rotavirus infection of human epithelial cells generates a distinct hyperphosphorylated form of keratin 8. Exp. Cell Res. **219:**348–357.
22. **Louvard, D., M. Kedinger, and H. P. Hauri.** 1992. The differentiating intestinal epithelial cell: establishment and maintenance of functions through interactions between cellular structures. Annu. Rev. Cell Biol. **8:**157–195.
23. **Matter, K., and I. Mellman.** 1994. Mechanism of cell polarity: sorting and transport in epithelial cells. Curr. Opin. Cell Biol. **6:**545–554.
24. **Mattion, N. M., J. Cohen, C. Aponte, and M. K. Estes.** 1992. Characterization of an oligomerization domain and RNA-binding properties on rotavirus nonstructural protein NS34. Virology **190:**68–83.
25. **Michelangeli, F., M.-C. Ruiz, J. R. Del Castillo, J. E. Ludert, and F. Liprandi.** 1991. Effect of rotavirus infection on intracellular calcium homeostasis in cultured cells. Virology **181:**520–527.
26. **Morris, A. P., J. K. Scott, J. M. Ball, C. Q. Zeng, W. K. O'Neal, and M. K. Estes.** 1999. NSP4 elicits age-dependent diarrhea and Ca^{2+}-mediated I^- influx into intestinal crypts of CF mice. Am. J. Physiol. **277:**G431–G444.
27. **Nilsson, M., C. H. V. Bonsdorff, K. Weclewicz, J. Cohen, and L. Svensson.** 1998. Assembly of viroplasm and virus-like particles of rotavirus by a Semliki Forest virus replicon. Virology **242:**255–265.
28. **Nishida, E., and H. Sakai.** 1977. Calcium-sensitivity of the microtubule reassembly system. Difference between crude brain extract and purified microtubular proteins. J. Biochem. (Tokyo) **82:**303–306.
29. **O'Brien, E. T., E. D. Salmon, and H. P. Erickson.** 1997. How calcium causes microtubule depolymerization. Cell Motil. Cytoskelet. **36:**125–135.
30. **Perez, J. F., M. C. Ruiz, M. E. Chemello, and F. Michelangeli.** 1999. Characterization of a membrane calcium pathway induced by rotavirus infection in cultured cells. J. Virol. **73:**2481–2490.
31. **Pinto, M., S. Robine-Leon, M. D. Appay, M. Kedinger, N. Triadou, E. Dussaulx, B. Lacroix, P. Simon-Assman, K. Haffen, J. Fogh, and A. Zweibaum.** 1983. Enterocyte-like differentiation and polarization of the human colon carcinoma cell line Caco-2 in culture. Biol. Cell **47:**323–330.
32. **Salas, P. J. I., M. L. Rodriguez, A. L. Viciana, D. E. Vegas-Salas, and H. P. Hauri.** 1997. The apical submembrane cytoskeleton participates in the organization of the apical pole in epithelial cells. J. Cell Biol. **137:**359–375.
33. **Sheth, R., J. Anderson, T. Sato, B. Oh, S. J. Hempson, E. Rollo, E. R. Mackow, and R. D. Shaw.** 1996. Rotavirus stimulates IL-8 secretion from cultured epithelial cells. Virology **221:**251–259.
34. **Superti, F., M. G. Ammendolia, A. Tinari, B. Bucci, A. M. Giammarioli, G. Rainaldi, R. Rivabene, and G. Donelli.** 1996. Induction of apoptosis in HT-29 cells infected with SA-11 rotavirus. J. Med. Virol. **50:**325–334.
35. **Svensson, L., B. B. Finlay, D. Bass, C.-H. von Bonsdorff, and H. B. Greenberg.** 1991. Symmetric infection of rotavirus on polarized human intestinal epithelial (Caco-2) cells. J. Virol. **65:**4190–4197.
36. **Tian, P., M. K. Estes, Y. Hu, J. M. Ball, C. Q. Y. Zeng, and W. P. Schilling.** 1995. The rotavirus nonstructural glycoprotein NSP4 mobilizes Ca^{2+} from the endoplasmic reticulum. J. Virol. **69:**5763–5772.
37. **Tian, P., Y. Hu, W. P. Shilling, D. A. Lindsay, J. Eiden, and M. K. Estes.** 1994. The nonstructural glycoprotein of rotavirus affects intracellular calcium levels. J. Virol. **68:**251–257.
38. **Tran, P. T., P. Joshi, and E. D. Salmon.** 1997. How tubulin subunits are lost from the shortening ends of microtubules. J. Struct. Biol. **118:**107–118.

39. **Tsien, R. Y., T. Pozzan, and T. J. Rink.** 1982. Calcium homeostasis in intact lymphocytes: cytoplasmic free calcium monitored with a new, intracellularly trapped fluorescent indicator. J. Cell Biol. **94:**325–334.
40. **Weclewicz, K., K. Kristensson, and L. Svensson.** 1994. Rotavirus causes selective vimentin reorganization in monkey kidney CV-1 cells. J. Gen. Virol. **75:**3267–3271.
41. **Weclewicz, K., L. Svensson, M. Billger, K. Holmberg, M. Wallin, and K. Kristensson.** 1993. Microtubule-associated protein 2 appears in axons of cultured dorsal root ganglia and spinal cord neurons after rotavirus infection. J. Neurosci. Res. **36:**173–182.
42. **Weisenberg, R. C.** 1972. Microtubule formation in vitro in solutions containing low calcium concentrations. Science **177:**1104–1105.
43. **Wollner, D. A., and W. J. Nelson.** 1992. Establishing and maintaining epithelial cell polarity. Roles of protein sorting, delivery, and retention. J. Cell Sci. **102:**185–190.
44. **Yano, T., T. Tokui, Y. Nishi, K. Nishizawa, M. Shibata, K. Kikuchi, S. Tsuiki, T. Yamauchi, and M. Inagaki.** 1991. Phosphorylation of keratin intermediate filaments by protein kinase C, by calmodulin-dependent protein kinase and by cAMP-dependent protein kinase. Eur. J. Biochem. **197:** 281–290.